Th P6 15

A New Wave Equation Based Source Location Method with Full-waveform Inversion

Z. Wu* (KAUST), T. Alkhalifah (KAUST)

Summary

Locating the source of a passively recorded seismic event is still a challenging problem, especially when the velocity is unknown. Many imaging approaches to focus the image do not address the velocity issue and result in images plagued with illumination artifacts. We develop a waveform inversion approach with an additional penalty term in the objective function to reward the focusing of the source image. This penalty term is relaxed early to allow for data fitting, and avoid cycle skipping, using an extended source. At the later stages the focusing of the image dominates the inversion allowing for high resolution source and velocity inversion. We also compute the source location explicitly and numerical tests show that we obtain good estimates of the source locations with this approach.

Introduction

Hydraulic fracturing is a widely used method in oil and gas extraction, especially in those reservoirs with dense rock formations such as shale. Locating the resulting fracturing effects using passive seismic acquisition is important to the hydraulic fracturing process. There are two general categories of approaches used to find the seismic source location. One group of methods are based on traveltime picks of either P-wave or S-wave arrivals (Waldhauser and Ellsworth, 2000; Eisner et al., 2009). These methods can explicitly give the source locations. However, they require picking the arrivals and rely on the high frequency asymptotic approximation of the wavefields, which will eventually lead to incorrect source locations with noisy data in complex areas. The other group of methods are based on solving the wave equation to focus the source, similar migration techniques, such as time reverse migration(Artman et al., 2010). These methods use the full wavefield to help locate the source. However, they usually do not give the explicit source location, instead they only provide an image of the source to indicate the possible source location. Also, these methods might suffer from artifacts in the source image, due to poor illumination. Using wave equation methods to obtain an artifact-free source image, which provides explicit source location, is still an active research topic. In this abstract, we use the wave equation in an optimization problem in which we invert for a source image that fits the data. In doing so we add an additional penalty term to the conventional data fitting misfit, which tries to enforce a focused source image. We use such an optimization problem to invert for the velocity model as well. However, the key feature of the approach is its explicit determination of the source location coordinates.

Theory

Standard full-waveform inversion (FWI) for a point source, represented by the Dirac delta function, $\delta(x-x_s)$, located at x_s, with a source wavelet given in the frequency domain by f, can be formulated as the following optimization problem

$$\min_{v,x_s,f(\omega)} \sum_{\omega} ||Cp(\omega)-g(\omega)||_{l^2}^2, \;\; s.t. \;\; S[v,\omega]p(\omega) = f(\omega)\delta(x-x_s), \tag{1}$$

where v is P-wave velocity and $S[v,\omega]$ is the discrete Helmholtz equation given in matrix form,as a function of angular frequency, ω. The operator C constrains the modeled wavefield, $p(\omega)$, to the receiver positions, with $g(\omega)$ representing the observed data. Here, we assume the source is a point source in space. Also, we assume that the source can be expressed as the multiplication of its time and space functions. We use l^2 norm to measure the difference between the modeled data and the observed data, for simplicity. More advanced Norms, such as the source independent objective function(Wang and Alkhalifah, 2016) can also be used. Unfortunately, the optimization problem (1) is highly nonlinear and suffers from cycle skipping. As a result, with this optimization problem we can easily fall into a local minimum near the initial velocity when using gradient based local optimization methods. An additional source of nonlinearity comes from the unknown source location and source wavelet. In order to mitigate the cycle skipping problem, and similar to Huang et al. (2016) for the active source case, we introduce a general source space function $w(x)$, and solve the following extended optimization problem instead

$$\min_{v,x_s,f(\omega),w(x)} \sum_{\omega} ||Cp(\omega)-g(\omega)||_{l^2}^2, \;\; s.t. \;\; S[v,\omega]p(\omega) = f(\omega)w(x). \tag{2}$$

In this case, the assumption of point source has been relaxed. This will help to fit the data better even with an inaccurate velocity, and thus, (2) dooes not admit a unique solution. However, based on our assumption, the generalized source space function $w(x)$ should end up being a δ function centered at the exact source location when the velocity is accurate. So to obtain a unique solution, we add some penalty term on w away from a δ function. Thus, similar to Shen and Symes (2008) and Huang et al. (2016), we use the following optimization problem

$$\min_{v,x_s,f(\omega),w(x)} \sum_{\omega} ||Cp(\omega)-g(\omega)||_{l^2}^2 + \alpha\frac{\sum_x |x-x_s|^2 w(x)^2}{\sum_x w(x)^2}, \;\; s.t. \;\; S[v,\omega]p(\omega) = f(\omega)w(x). \tag{3}$$

The function $\frac{\sum_x |x-x_s|^2 w(x)^2}{\sum_x w(x)^2}$ measures the focusing property of w to x_s. When $w(x)$ is given by a δ function centered at x_s, this penalty term is zero. Thus, the new optimization problem admits the same unique

solution as the optimization (1). The weight parameter α is user defined. When we choose α to be small, it means that we want to approximate the data more accurately with an extended source to avoid cycle skipping. This is needed when the velocity is far from accurate. For large α, we start to force the source function to be a delta function and start to focus on the high resolution aspects of the velocity model and the source location. To solve the above mentioned optimization problem (3), we propose the following nested scheme:

$$\min_{v}\min_{w(x)} J = \left(\sum_{\omega}\min_{f(\omega)}||Cp(\omega)-g(\omega)||_{l^2}^2\right)+\alpha\min_{x_s}\frac{\sum_x|x-x_s|^2w(x)^2}{\sum_x w(x)^2},\ \ s.t.\ \ S[v,\omega]p(\omega)=f(\omega)w(x). \tag{4}$$

For each given $v, w(x)$, the optimal x_s can be analytically obtained from

$$x_s = \frac{\sum_x w(x)^2 x}{\sum_x w(x)^2}. \tag{5}$$

Since it is just a two dimensional problem, the best $f(\omega)$ can be easily computed using the following relation

$$f(\omega) = \frac{< Cp(\omega), g(\omega) >_{l^2}}{< Cp(\omega), Cp(\omega) >_{l^2}}. \tag{6}$$

Here $< \cdot,\cdot >_{l^2}$ is the inner product of two complex vectors using the l^2 norm. After that, for each given v, we solve the optimization problem (4) to get the best $w(x)$ using the gradient

$$\frac{\partial J}{\partial w} = \left(\sum_{\omega} Re\left(f\bar{\lambda}(\omega)\right)\right)+2\alpha w(x)\left(\frac{|x-x_s|^2}{\sum_x w(x)^2}-\frac{\sum_x|x-x_s|^2w(x)^2}{(\sum_x w(x)^2)^2}\right). \tag{7}$$

Here, $\lambda = S[v,\omega]^{-T}(C^T(Cp-g))$ is the adjoint wavefield. At last, the gradient with respect to velocity v can be easily obtained by adjoint state method as

$$\frac{\partial J}{\partial v} = Re\left(< \frac{\partial S[v,\omega]}{\partial v}p, \lambda >_{l^2}\right). \tag{8}$$

One advantage of this approach is that it can provide a prediction of the source coordinates directly, as shown in (5), which is an additional feature not accessible in most wave equation based imaging. Also, since we relax the Dirac delta function requirement, the observed data can be approximated more accurately, which allows us to avoid cycle skipping.

Numerical examples

Our first example is a simple constant velocity model meant to highlight some of the features of the proposed objective function. The survey area is 4.25 km by 10 km with a sampling rate of 0.025 km by 0.025 km. The exact source is located at the bottom, specifically at coordinate location (3.375 km, 5 km). All grid points at depth level 0.875 km act as receivers. We first generate the exact data with 16 frequencies starting from 3.5 Hz to 7.25 Hz. The true velocity is 2 km/s. We calculate the objective function for different velocities ranging from 1.5 km/s to 2.5 km/s. The objective function as a function of constant velocities is shown in Figure 1(a). As we can see from Figure 1(a), even though we have included the source position inversion, the relative objective function has only one local minimum, which is the global minimum, located at 2 km/s. From Figure 2(a) and 2(b), we can see that the estimated source location with different velocities. To compare, we plot the standard FWI objective function with an exact source location and exact wavelet in Figure 1(b). Even though we assume that we know the exact source information, the standard FWI suffers from the local minima problem, as shown in Figure 1(b).

Our next example is the Marmousi model. The exact velocity is shown in Figure 3(a). We use, equally distributed in frequency, data with 16 frequencies ranging between 5 Hz and 9 Hz. We invert for all frequencies simultaneously. The grid spacing for the model is 0.025 km in both directions. The exact source is located at (z=1.75 km, x=4.6 km) and all the points on the surface are serving as receivers. In

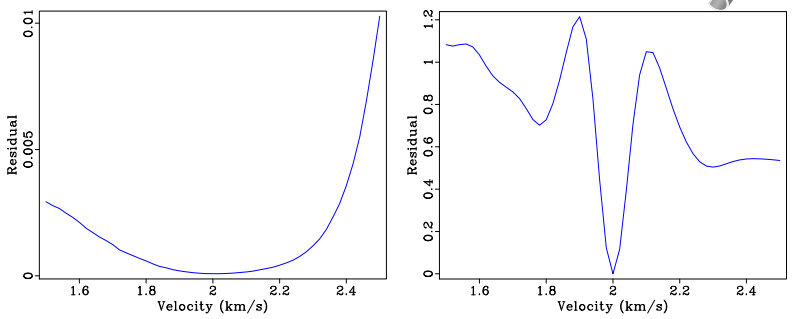

(a) (b)

Figure 1 *The comparison of objective function (a) New objective function with the including of source estimation. (b) Standard FWI objective with exact source wavelet and position.*

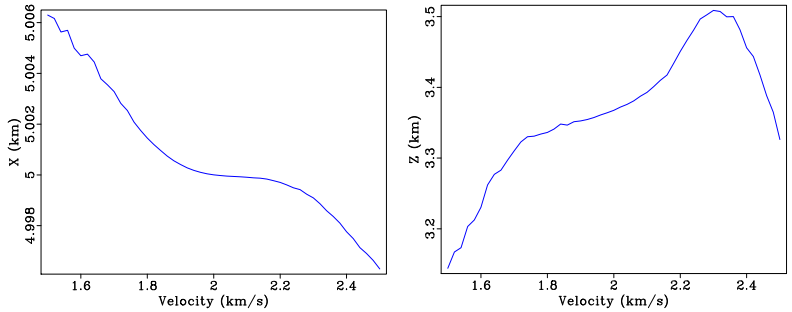

(a) (b)

Figure 2 *The estimated source location for different velocity. (a) X coordinate (b) Z coordinate.*

our first test, we invert for the source only using the exact velocity. The inverted source space function is shown in Figure 3(b). As we can see from Figure 3(b), the inverted source is located at the exact position and our estimated source location is at (z=1.745 km, x=4.599 km), very close to the true location. Figures 3(c) and 3(d) show the inverted source image profiles at the exact source location. As expected we have higher lateral resolution in the source. As we can see from Figure 3(b), there are no artifacts in the inverted source image. Next, we consider inverting the velocity and source image, simultaneously. The initial velocity is linearly increasing shown in Figure 4(a). The data are generated using the exact velocity shown in Figure 3(a) with 16 frequencies ranging from 1 Hz to 5 Hz. The exact source is located at (z=2.5 km, x=4.6 km). We obtain the inverted velocity shown in Figure 4(b) and the inverted source image shown in Figure 4(c). The inverted source location is at (z=2.21 km, 4.84 km), which is close to the exact one in about less than a half of the wavelength of the maximum frequency used.

Conclusions

We generalized the objective of FWI to focus an unknown source image and wavelet by relaxing the delta function assumption of the point source, thus mitigating the the cycle skipping problem for an inaccurate velocity model. A penalty term used heavily at later iterations enforces the focusing of the source image, based on a point source assumption. The resulting algorithm provides explicit information on the source location, and the inverted source image is free from illumination artifacts plaguing conventional wave equation based source image methods. The approach can invert for the source location and velocity model, simultaneously.

Acknowledgements

We thank KAUST for its support and we thank the SWAG group for collaborative environment. We thank Guanghui Huang and Hanchen Wang for the useful discussions. For computer time, this research used the resources of the Supercomputing Laboratory at King Abdullah University of Science and Technology (KAUST) in Thuwal, Saudi Arabia.

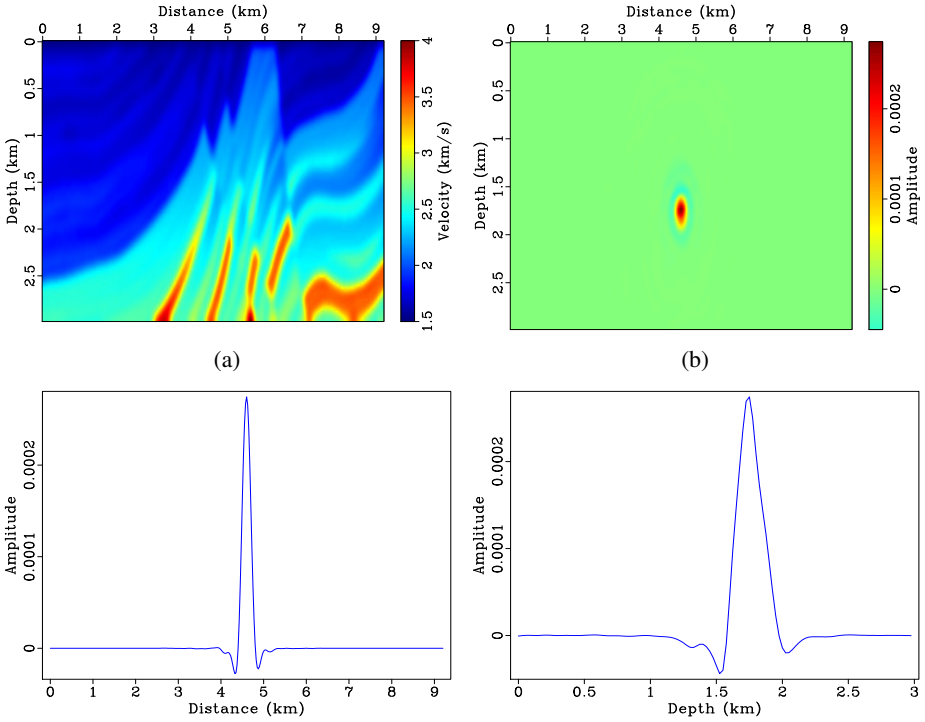

Figure 3 *The exact velocity (a) and the inverted source image using the exact velocity (b). The inverted source profile at the exact source location((c) x profile and (d) z profile).*

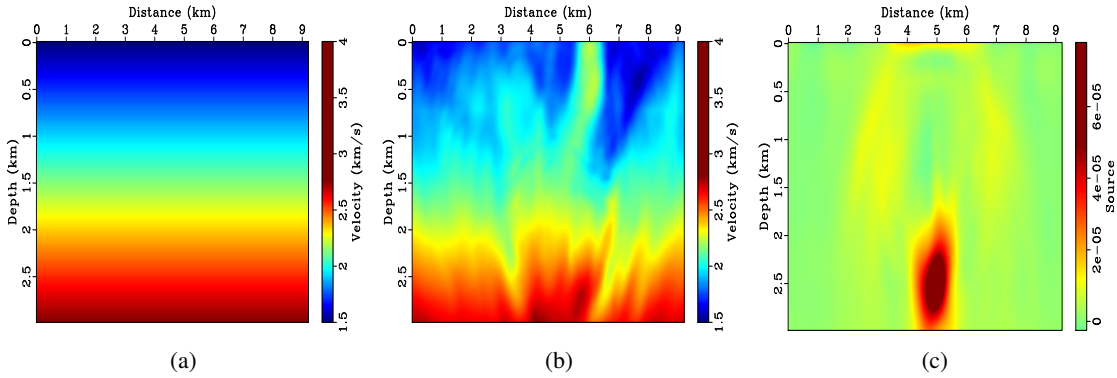

Figure 4 *(a) The initial velocity. (b) The inverted velocity. (c) The inverted source image.*

References

Artman, B., Podladtchikov, I. and Witten, B. [2010] Source location using time-reverse imaging. *Geophysical Prospecting*, **58**(5), 861–873.

Eisner, L., Duncan, P.M., Heigl, W.M. and Keller, W.R. [2009] Uncertainties in passive seismic monitoring. *The Leading Edge*, **28**(6), 648–655.

Huang, G., Symes, W. and Nammour, R. [2016] Matched source waveform inversion: Space-time extension. In: *86st Ann. Internat. Mtg, SEG Expanded Abstracts*. 1426–1431.

Shen, P. and Symes, W.W. [2008] Automatic velocity analysis via shot profile migration. *GEOPHYSICS*, **73**(5), VE49–VE59.

Waldhauser, F. and Ellsworth, W.L. [2000] A Double-Difference Earthquake Location Algorithm: Method and Application to the Northern Hayward Fault, California. *Bulletin of the Seismological Society of America*, **90**(6), 1353–1368.

Wang, H. and Alkhalifah, T. [2016] Microseismic imaging using a source-independent full-waveform inversion method. In: *88st Ann. Internat. Mtg, SEG Expanded Abstracts*. 2596–2600.